Proceedings of the Korea Nuclear Society Spring Meeting

Cheju, Korea, May 2001

Unified Nodal Method for Transient Analytic Function Expansion Nodal Calculations

Hyun Chul Lee and Chang Hyo Kim

Seoul National University

San 56-1 Shillim-dong, Kwanak-gu

Seoul, Korea 151-742

Abstract

The unified nodal method (UNM) for transient analytic function expansion nodal(AFEN) method solution to two-group diffusion equation in rectangular geometry is newly formulated. The performance of the new UNM is examined through the solution to the OECD/NEA PWR transient problem designated A1. It is shown that the UNM for the transient AFEN calculations outperform the popular transverse integrated nodal methods (TINM) like the nodal expansion method (NEM) and the analytic nodal method (ANM) in prediction accuracy at the sacrifice of the computational time.

1. Introduction

Recently we presented a unified nodal method (UNM) formulation for the analytic function expansion nodal (AFEN) method solutions to static two-group diffusion equations in rectangular geometry[1] and demonstrated that the UNM formulation results in exactly the same solutions as the AFEN method solutions in terms of the three-dimensional (3-D) static IAEA benchmark problem. The purpose of this paper is to present the UNM formulation for the transient AFEN method solutions to transient neutronics problems in the rectangular geometry and examine its computational effectiveness in terms of 3-D transient solutions to the well-known OECD/NEA kinetics benchmark problem[2].

2. UNM Formulation for Transient AFEN Solution

UNM formulation for the transient AFEN option requires determining intranodal flux distribution from a set of the time-dependent 2-G diffusion equations for a given spatial node *m*

$$\frac{1}{v_g}\frac{\partial \phi_g^m(\mathbf{r},t)}{\partial t} = \nabla\cdot D_g^m(t)\nabla\phi_g^m(\mathbf{r},t) - \Sigma_{rg}^m(t)\phi_g^m(\mathbf{r},t) + \frac{\chi_g}{k_{eff}}(1-\beta)\sum_{g'=1}^{2} \nu\Sigma_{fg'}^m(t)\phi_{g'}^m(\mathbf{r},t) + \sum_{\substack{g'=1\\ g'\neq g}}^{2}\Sigma_{sgg'}^m(t)\phi_{g'}^m(\mathbf{r},t) + \chi_g\sum_{d=1}^{6}\lambda_d C_d^m(\mathbf{r},t);\quad g=1,2 \tag{1a}$$

$$\frac{\partial C_d^m(\mathbf{r},t)}{\partial t} = \frac{\beta}{k_{eff}} \sum_{g'=1}^{2} \nu\Sigma_{fg'}^m(t)\phi_{g'}^m(\mathbf{r},t) - \lambda_d C_d^m(\mathbf{r},t); \quad d = 1,2,\Lambda\ ,6 \tag{1b}$$

$\phi_g^m(\mathbf{r},t)$ and $C_d^m(\mathbf{r},t)$ are the group g flux and the type d delayed neutron precursor density, respectively. The other notations are standard.

The efficiency can be enhanced by applying exponential transform :

$$\phi_g^m(\mathbf{r},t) = e^{\omega t}\psi_g^m(\mathbf{r},t).$$

A fully implicit temporal integration of Eq. (1) over the time interval between (t_{n-1}, t_n) leads to

$$\begin{aligned} -\nabla\cdot D_g^{(n)}(t)\nabla\phi_g^{(n)}(\mathbf{r}) + \left(\frac{\omega_g^{(n)}\Delta t + 1}{v_g\Delta t} + \Sigma_{rg}^{(n)}\right)\phi_g^{(n)}(\mathbf{r}) - \frac{e^{\omega_g^{(n)}\Delta t}}{v_g\Delta t}\phi_g^{(n-1)}(\mathbf{r}) \\ = \frac{\chi_g}{k_{eff}}\left(1-\beta+\sum_{d=1}^{6}\lambda_d\beta_d\frac{1-e^{-\left(\lambda_d+\overline{\omega}^{(n)}\right)\Delta t}}{\lambda_d+\overline{\omega}^{(n)}}\right)\sum_{g'=1}^{2}\nu\Sigma_{fg'}^{(n)}\phi_{g'}^{(n)}(\mathbf{r}) \\ + \sum_{\substack{g'=1\\ g'\neq g}}^{2}\Sigma_{sgg'}^{(n)}\phi_{g'}^{(n)}(\mathbf{r}) + \chi_g\sum_{d=1}^{6}\lambda_d e^{-\lambda_d\Delta t}C_d^{(n-1)}(\mathbf{r}); \quad g = 1,2 \end{aligned} \tag{2a}$$

$$C_d^{(n)}(\mathbf{r}) \approx e^{-\lambda_d\Delta t}C_d^{(n-1)}(\mathbf{r}) + \frac{\beta_d}{k_{eff}}\left(\frac{1-e^{-\left(\lambda_d+\overline{\omega}^{(n)}\right)\Delta t}}{\lambda_d+\overline{\omega}^{(n)}}\right)\sum_{g'=1}^{2}\nu\Sigma_{fg'}^{(n)}\phi_{g'}^{(n)}(\mathbf{r}); \quad d = 1,2,\Lambda\ ,6 \tag{2b}$$

We dropped the superscript m in Eq. (2) for simplicity of notation. The fission source term of Eq. (1b) is approximated by[3]

$$\sum_{g'=1}^{2}\nu\Sigma_{fg'}^m(t)\phi_{g'}^m(\mathbf{r},t) \approx e^{\overline{\omega}^{(n)}t}\sum_{g'=1}^{2}\nu\Sigma_{fg'}^m(t)\psi_{g'}^m(\mathbf{r},t) \tag{3}$$

where $\overline{\omega}^{(n)} = \dfrac{\omega_1^{(n)} + \omega_2^{(n)}}{2}$

Equation (2) is an inhomogeneous equation that one may use to determine the intranodal flux distribution at each time step, as in reference 3. In order to determine the intranodal flux in the same way as in the static case,

however, we introduce following approximations;

$$\omega_g^{(n)} = \frac{1}{\Delta t}\ln\left(\frac{\bar{\phi}_g^{(n)}}{\bar{\phi}_g^{(n-1)}}\right) \tag{4a}$$

$$\frac{\phi_{gu}^{(n-1)}(u)}{\bar{\phi}_g^{(n-1)}} \approx \frac{\phi_{gu}^{(n)}(u)}{\bar{\phi}_g^{(n)}} \tag{4b}$$

$$\frac{C_{du}^{(n-1)}(u)}{\bar{C}_d^{(n-1)}} \approx \frac{\sum_{g'=1}^{2} \nu\Sigma_{fg'}^{(n)} \bar{\phi}_{g'u}^{(n)}(u)}{\sum_{g'=1}^{2} \nu\Sigma_{fg'}^{(n)} \bar{\phi}_{g'}^{(n)}} \tag{4c}$$

Substituting Eq. (4) into Eq. (2a), we have

$$\begin{aligned} &-\nabla\cdot D_g^{(n)}(t)\nabla\phi_g^{(n)}(\mathbf{r}) + \left(\frac{\omega_g^{(n)}}{v_g} + \Sigma_{rg}^{(n)}\right)\phi_g^{(n)}(\mathbf{r}) \\ &\quad = \frac{\chi_g}{k_{eff}}\left(1-\beta+\sum_{d=1}^{6} W_d^{(n)}\right)\sum_{g'=1}^{2} \nu\Sigma_{fg'}^{(n)}\phi_{g'}^{(n)}(\mathbf{r}) + \sum_{\substack{g'=1 \\ g'\neq g}}^{2} \Sigma_{sgg'}^{(n)}\phi_{g'}^{(n)}(\mathbf{r}); \quad g = 1,2 \end{aligned} \tag{5}$$

Where $$W_d^{(n)} = \frac{\lambda_d e^{-\lambda_d \Delta t_n}\bar{C}_d^{(n-1)}}{\frac{1}{k_{eff}}\sum_{g'=1}^{2} \nu\Sigma_{fg'}^{(n)}\bar{\phi}_{g'}^{(n)}} + \lambda_d\beta_d\left(\frac{1-e^{-\left(\lambda_d+\bar{\omega}^{(n)}\right)\Delta t_n}}{\lambda_d+\bar{\omega}^{(n)}}\right)$$

Equation (5) can be put

$$\nabla^2\boldsymbol{\phi}^{(n)}(\mathbf{r}) - \left(\mathbf{D}^{(n)}\right)^{-1}\mathbf{A}^{(n)}\boldsymbol{\phi}^{(n)}(\mathbf{r}) = \mathbf{0}, \tag{6}$$

where $\boldsymbol{\phi}^{(n)}$ = 2-dimensional column vector $(\phi_1^{(n)}, \phi_2^{(n)})$. The elements of the 2x2 matrix $\mathbf{A}^{(n)}$ are given by

$$A_{11}^{(n)} = \left(\frac{\omega_1^{(n)}}{v_1} + \Sigma_{r1}^{(n)}\right) - \frac{1}{k_{eff}}\left(1-\beta+\sum_{d=1}^{6} W_d^{(n)}\right)\nu\Sigma_{f1}^{(n)}, \qquad A_{12}^{(n)} = -\frac{1}{k_{eff}}\left(1-\beta+\sum_{d=1}^{6} W_d^{(n)}\right)\nu\Sigma_{f2}^{(n)}$$

$$A_{21}^{(n)} = -\Sigma_{s21}^{(n)}, \qquad A_{22}^{(n)} = \left(\frac{\omega_2^{(n)}}{v_2} + \Sigma_{r2}^{(n)}\right)$$

Equation (6) has exactly the same form as the 2-G equation used for determining the intranodal flux distribution in the static AFEN calculation. $\mathbf{A}^{(0)}$ characterizes the 2-G equation at the initial steady state and is given by

$$\mathbf{A}^{(0)} = \begin{pmatrix} \Sigma_{r1}^{(0)} - \dfrac{1}{k_{eff}} \nu\Sigma_{f1}^{(0)} & -\dfrac{1}{k_{eff}} \nu\Sigma_{f2}^{(0)} \\ -\Sigma_{s21}^{(0)} & \Sigma_{r2}^{(0)} \end{pmatrix}$$

Eq. (6) can be diagonalized into the form

$$\nabla^2 \boldsymbol{\xi}^{(n)}(\mathbf{r}) - \hat{\mathbf{A}}^{(n)} \boldsymbol{\xi}^{(n)}(\mathbf{r}) = \mathbf{0}, \tag{7}$$

where

$$\boldsymbol{\xi}^{(n)}(\mathbf{r}) = \left(\mathbf{R}^{(n)}\right)^{-1} \boldsymbol{\phi}^{(n)}(\mathbf{r}),$$

$$\hat{\mathbf{A}}^{(n)} = \left(\mathbf{R}^{(n)}\right)^{-1} \left(\mathbf{D}^{(n)}\right)^{-1} \mathbf{A}^{(n)} \mathbf{R}^{(n)} = \begin{pmatrix} \lambda_1^{(n)} & 0 \\ 0 & \lambda_2^{(n)} \end{pmatrix}.$$

The similarity transform matrix $\mathbf{R}^{(n)}$ can be defined in the same way as static case.
As shown in reference 4, the general solution of Eq. (7) is

$$\xi^{(n)}(x,y,z) = \sum_{i=0}^{\infty} \left[\tilde{A}_{ip}^{(n)} \sinh\left(\alpha_{ipx}^{(n)} x + \alpha_{ipy}^{(n)} y + \alpha_{ipz}^{(n)} z\right) + \tilde{B}_{ip}^{(n)} \cosh\left(\alpha_{ipx}^{(n)} x + \alpha_{ipy}^{(n)} y + \alpha_{ipz}^{(n)} z\right) \right] \tag{8}$$

Equation (8) provides many different approximations for the intranodal flux distribution on which the AFEN is based. One such approximation is given by

$$\begin{aligned} \xi_p^{(n)}(x,y,z) \cong\ & A_{p0}^{(n)} + A_{1px}^{(n)} \sinh\left(\kappa_p^{(n)} x\right) + A_{2px}^{(n)} \cosh\left(\kappa_p^{(n)} x\right) \\ & + A_{1py}^{(n)} \sinh\left(\kappa_p^{(n)} y\right) + A_{2py}^{(n)} \cosh\left(\kappa_p^{(n)} y\right) \\ & + A_{1pz}^{(n)} \sinh\left(\kappa_p^{(n)} z\right) + A_{2pz}^{(n)} \cosh\left(\kappa_p^{(n)} z\right) \\ & + B_{1pz}^{(n)} \sinh\left(\mu_p^{(n)} x\right) \sinh\left(\mu_p^{(n)} y\right) + B_{2pz}^{(n)} \sinh\left(\mu_p^{(n)} x\right) \cosh\left(\mu_p^{(n)} y\right) \\ & + B_{3pz}^{(n)} \cosh\left(\mu_p^{(n)} x\right) \sinh\left(\mu_p^{(n)} y\right) + B_{4pz}^{(n)} \cosh\left(\mu_p^{(n)} x\right) \cosh\left(\mu_p^{(n)} y\right), \\ & + B_{1px}^{(n)} \sinh\left(\mu_p^{(n)} y\right) \sinh\left(\mu_p^{(n)} z\right) + B_{2px}^{(n)} \sinh\left(\mu_p^{(n)} y\right) \cosh\left(\mu_p^{(n)} z\right) \\ & + B_{3px}^{(n)} \cosh\left(\mu_p^{(n)} y\right) \sinh\left(\mu_p^{(n)} z\right) + B_{4px}^{(n)} \cosh\left(\mu_p^{(n)} y\right) \cosh\left(\mu_p^{(n)} z\right) \\ & + B_{1py}^{(n)} \sinh\left(\mu_p^{(n)} z\right) \sinh\left(\mu_p^{(n)} x\right) + B_{2py}^{(n)} \sinh\left(\mu_p^{(n)} z\right) \cosh\left(\mu_p^{(n)} x\right) \\ & + B_{3py}^{(n)} \cosh\left(\mu_p^{(n)} z\right) \sinh\left(\mu_p^{(n)} x\right) + B_{4py}^{(n)} \cosh\left(\mu_p^{(n)} z\right) \cosh\left(\mu_p^{(n)} x\right) \end{aligned} \tag{9}$$

where

$$\mu_p^{(n)} = \frac{\kappa_p^{(n)}}{\sqrt{2}}. \qquad \kappa_p^{(n)} = \sqrt{\lambda_p^{(n)}}$$

The intranodal flux distribution above contains 19 expansion coefficients. They can be determined by 19 nodal unknowns per rectangular prism node per neutron group; 1 node average flux ($\overline{\xi}_p$), 6 surface average fluxes ($\xi_{pus}; u = x, y, z; s = l, r$), and 12 edge fluxes ($\xi_{pu}^{(i)}; u = x, y, z; i = 1,2,3,4$). To derive nodal coupling relations among these nodal unknowns, the AFEN method uses nodal balance condition, current continuity conditions at six nodal interfaces, and the twelve corner point balance (CPB) conditions. The UNM formulation uses the same CPB conditions to get the twelve CPB equations for edge fluxes. To derive the rest of coupling relations, however, the UNM follows the nodal expansion method (NEM) procedure based on the transverse integration of Eq. (7), as shown below.

First, let us note that integration of Eq. (5) over each rectangular prism node results in the nodal balance relation,

$$\begin{aligned} &\sum_{u=x,y,z} \frac{1}{a_u}\left(J_{gur}^{(n)} - J_{gul}^{(n)}\right) + \left(\frac{\omega_g^{(n)}}{v_g} + \Sigma_{rg}^{(n)}\right)\overline{\phi}_g^{(n)} \\ &\qquad = \frac{\chi_g}{k_{eff}}\left(1 - \beta + \sum_{d=1}^{6} W_d^{(n)}\right)\sum_{g'=1}^{2} \nu\Sigma_{fg'}^{(n)}\overline{\phi}_{g'}^{(n)} + \sum_{\substack{g'=1 \\ g'\neq g}}^{2} \Sigma_{sgg'}^{(n)}\overline{\phi}_{g'}^{(n)} \end{aligned} \tag{10}$$

Equation (10) contains $\overline{\phi}_g^{(n)}$ and $J_{gus}^{(n)}$ as unknowns. Therefore its solution requires additional relations between $\overline{\phi}_g^{(n)}$ and $J_{gus}^{(n)}$. To get them in the UNM principle, we use the transverse integrated 1-D equations of Eq. (7),

$$\frac{d^2}{du^2}\xi_{pu}(u) - \lambda_p \xi_{pu}(u) = \hat{L}_{pu}(u), \tag{11}$$

where

$$\xi_{pu}(u) = \frac{1}{a_u a_w}\int_{-\frac{a_w}{2}}^{+\frac{a_w}{2}}\int_{-\frac{a_v}{2}}^{+\frac{a_v}{2}} \xi_p(u, v, w)\,dv\,dw$$

$$\hat{L}_{pu}(u) = -\frac{1}{a_u a_w}\int_{-\frac{a_w}{2}}^{+\frac{a_w}{2}}\int_{-\frac{a_v}{2}}^{+\frac{a_v}{2}}\left(\frac{\partial^2}{\partial v^2} + \frac{\partial^2}{\partial w^2}\right)\xi_p(u, v, w)\,dv\,dw$$

$\xi_{pu}(u)$ and $\hat{L}_{pu}(u)$ are the transverse integrated 1-D flux and the transverse leakage, respectively. Because of Eq. (9) for the intranodal flux, $\hat{L}_{pu}(u)$ can be expressed by

$$\hat{L}_{pu}(u) = \sum_{i=0}^{2} \hat{L}_{ipu} g_{ipu}\left(\frac{u}{a_u}\right), \tag{12}$$

where

$$g_{opu}(\tau) = 1,$$

$$g_{1pu}(\tau) = a_1 \sinh\left(2\tilde{\mu}_{pu}\tau\right),$$

$$g_{2pu}(\tau) = a_2 \cosh\left(2\tilde{\mu}_{pu}\tau\right) + b_2,$$

$$\tilde{\mu}_{pu} = \frac{\mu_p a_u}{2}.$$

The coefficients a_1, a_2, b_2 are determined so that $g_{1pu}\left(\pm 1/2\right) = \pm 1$, $g_{2pu}\left(\pm 1/2\right) = +1$, and $\int_{-1/2}^{+1/2} g_{ipu}(\tau) d\tau = 0 \ (i = 1,2)$. The $\hat{L}_{ipu} \ (i = 0,1,2)$ are given by corner point ($\xi_{pu}^{i}; u = x, y, z;$ $i = 1,2,3,4$), surface average (ξ_{pus} ; $u = x, y, z$; $s = r, l$), and node average value ($\overline{\xi}$) of $\xi_p(x, y, z)$. For example, $\hat{L}_{2pu}$ is given by

$$\begin{aligned}\hat{L}_{2pu} = {} & \hat{P}_{pv}\left[\xi_{pw}^{1} + \xi_{pw}^{2} + \xi_{pw}^{3} + \xi_{pw}^{4} + 4\overline{\xi} - 2\left(\xi_{pur} + \xi_{pul} + \xi_{pvr} + \xi_{pvl}\right)\right] \\ & + \hat{P}_{pw}\left[\xi_{pv}^{1} + \xi_{pv}^{2} + \xi_{pv}^{3} + \xi_{pv}^{4} + 4\overline{\xi} - 2\left(\xi_{pur} + \xi_{pul} + \xi_{pwr} + \xi_{pwl}\right)\right];\end{aligned}$$

$$\hat{P}_{pu} = \frac{1}{a_u^2} \frac{\tilde{\mu}_{pu}^2 \sinh\left(\tilde{\mu}_{pu}\right)}{\tilde{\mu}_{pu} \cosh\left(\tilde{\mu}_{pu}\right) - \sinh\left(\tilde{\mu}_{pu}\right)}, \ (p = 1,2) \tag{13}$$

Instead of using $\xi_{pu}(u)$ from direct integration of $\xi(u, v, w)$ over v and w, the UNM formulation uses the analytic solution of Eq. (11) which can be obtained by assuming the following expansion,

$$\xi_{pu}(u) = \sum_{i=0}^{4} \hat{C}_{ipu} f_{ipu}(u/a_u), \tag{14}$$

where the basis functions $f_{ipu}(\tau)$ are defined in reference 1.

The five expansion coefficients are determined by nodal balance condition, $\bar{\xi}_p = 1/a_u \int_{-a_u/2}^{+a_u/2} \xi_{pu}(u)du$, two conditions at two nodal surfaces, $\xi_{pu}(\pm a_u/2)$, and two weighted residual method (WRM) equations

$$\int_{-a_u/2}^{+a_u/2} f_{ipu}(u/a_u)[\text{Eq.(11) with } \xi_{pu}(u) \text{ in Eq. (14)}]du \quad (i = 1,2), \tag{15}$$

to find

$$\hat{\mathbf{C}}_{0u} = \bar{\boldsymbol{\xi}}_u, \tag{16}$$

$$\hat{\mathbf{C}}_{1u} = \frac{1}{2}\left[\boldsymbol{\xi}_u\left(+\frac{a_u}{2}\right) - \boldsymbol{\xi}_u\left(-\frac{a_u}{2}\right)\right], \tag{17}$$

$$\hat{\mathbf{C}}_{2u} = \frac{1}{2}\left[\boldsymbol{\xi}_u\left(+\frac{a_u}{2}\right) + \boldsymbol{\xi}_u\left(-\frac{a_u}{2}\right)\right] - \bar{\boldsymbol{\xi}}_u, \tag{18}$$

$$\hat{\mathbf{C}}_{3u} = \left(\hat{\mathbf{G}}_{3u}\hat{\mathbf{H}}_{3u}\right)^{-1}\left[\hat{\mathbf{A}}\hat{\mathbf{H}}_{3u}\hat{\mathbf{C}}_{1u} + \hat{\mathbf{L}}_{1u}\right], \tag{19}$$

$$\hat{\mathbf{C}}_{4u} = \left(\hat{\mathbf{G}}_{4u}\hat{\mathbf{H}}_{4u}\right)^{-1}\left[\hat{\mathbf{A}}\hat{\mathbf{H}}_{4u}\hat{\mathbf{C}}_{2u} + \hat{\mathbf{L}}_{2u}\right], \tag{20}$$

where $\hat{\mathbf{C}}_{iu}$ = 2-D column vector $\left(\hat{C}_{i1u}, \hat{C}_{i2u}\right)(i = 0,1,\text{K},4)$, $\bar{\boldsymbol{\xi}}$ = 2-D column vector $\left(\bar{\xi}_{1u}, \bar{\xi}_{2u}\right)$,

$$\hat{\mathbf{G}}_{iu} = \begin{pmatrix} \hat{G}_{i1u} & 0 \\ 0 & \hat{G}_{i2u} \end{pmatrix}, \hat{\mathbf{H}}_{iu} = \begin{pmatrix} \hat{H}_{i1u} & 0 \\ 0 & \hat{H}_{i2u} \end{pmatrix}, (i = 3,4) \tag{21}$$

The elements of $\hat{\mathbf{G}}_{iu}$ and $\hat{\mathbf{H}}_{iu}$ are given in reference 1.

The expansion coefficients determined above are related to node average flux and nodal surface average fluxes as follows;

$$\mathbf{C}_{0u} \equiv \mathbf{R}\hat{\mathbf{C}}_{0u} = \mathbf{R}\bar{\boldsymbol{\xi}}_u = \bar{\boldsymbol{\phi}}_u, \tag{22}$$

$$\mathbf{C}_{1u} \equiv \mathbf{R}\hat{\mathbf{C}}_{1u} = \frac{1}{2}\left[\boldsymbol{\phi}_u\left(+\frac{a_u}{2}\right) - \boldsymbol{\phi}_u\left(-\frac{a_u}{2}\right)\right], \tag{23}$$

$$\mathbf{C}_{2u} \equiv \mathbf{R}\hat{\mathbf{C}}_{2u} = \frac{1}{2}\left[\boldsymbol{\phi}_u\left(+\frac{a_u}{2}\right) + \boldsymbol{\phi}_u\left(-\frac{a_u}{2}\right)\right] - \bar{\boldsymbol{\phi}}_u, \tag{24}$$

$$\mathbf{C}_{3u} = \mathbf{R}\hat{\mathbf{C}}_{3u} = \mathbf{M}_{3u}^{-1}(\mathbf{M}_{1u}\mathbf{C}_{1u} + \mathbf{L}_{1u}) \tag{25}$$

$$\mathbf{C}_{4u} = \mathbf{R}\hat{\mathbf{C}}_{4u} = \mathbf{M}_{4u}^{-1}(\mathbf{M}_{2u}\mathbf{C}_{2u} + \mathbf{L}_{2u}) \tag{26}$$

where

$$\mathbf{M}_{1u} = \mathbf{R}\hat{\mathbf{A}}\hat{\mathbf{H}}_{3u}\mathbf{R}^{-1}, \quad \mathbf{M}_{3u} = \mathbf{D}\mathbf{R}\hat{\mathbf{G}}_{3u}\hat{\mathbf{H}}_{3u}\mathbf{R}^{-1}, \tag{27}$$

$$\mathbf{M}_{2u} = \mathbf{R}\hat{\mathbf{A}}\hat{\mathbf{H}}_{4u}\mathbf{R}^{-1}, \quad \mathbf{M}_{4u} = \mathbf{D}\mathbf{R}\hat{\mathbf{G}}_{4u}\hat{\mathbf{H}}_{4u}\mathbf{R}^{-1}, \tag{28}$$

$$\mathbf{L}_{iu} = \mathbf{D}\mathbf{R}\hat{\mathbf{L}}_{iu} \quad (i = 1,2) \tag{29}$$

From the definition of the partial currents,

$$\mathbf{j}_{us}^{\pm} = \frac{1}{4}\boldsymbol{\phi}_{us} \mp \frac{1}{2}\mathbf{D}\frac{d\boldsymbol{\phi}_{us}}{du} \quad (s = l, r), \tag{30}$$

and noting $\boldsymbol{\phi}_u(u) \equiv \mathbf{R}\boldsymbol{\xi}_u(u)$, one can relate the outgoing partial currents to the incoming partial currents by

$$\begin{aligned} \mathbf{j}_{ur}^{+} &= \mathbf{Q}_{0u}\left(6\bar{\boldsymbol{\phi}} - \mathbf{C}_{4u}\right) - \mathbf{Q}_{1u}\mathbf{C}_{3u} - \mathbf{Q}_{2u}\mathbf{j}_{ul}^{+} + \mathbf{Q}_{3u}\mathbf{j}_{ur}^{-} \\ \mathbf{j}_{ul}^{-} &= \mathbf{Q}_{0u}\left(6\bar{\boldsymbol{\phi}} - \mathbf{C}_{4u}\right) + \mathbf{Q}_{1u}\mathbf{C}_{3u} - \mathbf{Q}_{2u}\mathbf{j}_{ur}^{-} + \mathbf{Q}_{3u}\mathbf{j}_{ul}^{+} \end{aligned}, \tag{31}$$

where $\mathbf{j}_{us}^{\pm}$ = 2-D column vector $\left(j_{1us}^{\pm}, j_{2us}^{\pm}\right)$ and $\boldsymbol{\phi}_{us}$ = 2-D column vector $\left(\phi_{1us}, \phi_{2us}\right)$. They are the *u*-directed partial currents and 1-D fluxes, respectively, at the right surface (*s*=*r*) or at the left surface (*s*=*l*) of the node. The 2x2 diagonal matrices, $\mathbf{Q}_{ku}$ $(k = 0,1,2,3)$ are defined in reference 5. If one substitutes these equations into the nodal balance equation, Eq. (3), one finds that the node average flux is given by

$$\bar{\boldsymbol{\phi}} = \left(\mathbf{A} + 12\mathbf{Q}_0\right)^{-1}\mathbf{S}, \tag{32}$$

where

$$\mathbf{Q}_0 = \sum_{u=x,y,z} \frac{1}{a_u}\mathbf{Q}_{0u} \quad \mathbf{S} = \sum_{u=x,y,z} \frac{2\mathbf{Q}_{0u}\mathbf{C}_{4u} + \left(\mathbf{I} + \mathbf{Q}_{2u} - \mathbf{Q}_{3u}\right)\left(\mathbf{j}_{ur}^{-} + \mathbf{j}_{ul}^{+}\right)}{a_u}. \tag{33}$$

In deriving Eqs. (31) and (32), we used $\mathbf{J}_{us} = \mathbf{j}_{us}^{+} - \mathbf{j}_{us}^{-}$ (s=l,r). Equations (31) and (32) constitute the basic nodal coupling relations in the UNM formulation which have to be solved for $\overline{\boldsymbol{\phi}}$ and $\mathbf{j}_{us}^{\pm}\left(u = x, y, z; s = l, r\right)$. They are the same as those of the UNM formulation of the ANM[5] except for the fact that the diagonal matrices $\hat{\mathbf{G}}_{iu}$ and $\hat{\mathbf{H}}_{iu}$ (i=3,4) and vector $\mathbf{L}_{iu}$ (i=1,2) are defined differently. Because of Eq. (13) and Eq. (29), $\mathbf{L}_{iu}$ (i=1,2) in the AFEN option is given by nine unknown nodal fluxes of the given node;

$$\begin{aligned}\mathbf{L}_{1u} &= \mathbf{P}_v\left[\boldsymbol{\phi}_w^1 - \boldsymbol{\phi}_w^2 - \boldsymbol{\phi}_w^3 + \boldsymbol{\phi}_w^4 - 2\left(\boldsymbol{\phi}_{ur} - \boldsymbol{\phi}_{ul}\right)\right] \\ &\quad + \mathbf{P}_w\left[\boldsymbol{\phi}_v^1 + \boldsymbol{\phi}_v^2 - \boldsymbol{\phi}_v^3 - \boldsymbol{\phi}_v^4 - 2\left(\boldsymbol{\phi}_{ur} - \boldsymbol{\phi}_{ul}\right)\right],\end{aligned} \tag{34}$$

$$\begin{aligned}\mathbf{L}_{2u} &= \mathbf{P}_v\left[\boldsymbol{\phi}_w^1 + \boldsymbol{\phi}_w^1 + \boldsymbol{\phi}_w^1 + \boldsymbol{\phi}_w^1 + 4\overline{\boldsymbol{\phi}} - 2\left(\boldsymbol{\phi}_{ur} + \boldsymbol{\phi}_{ul} + \boldsymbol{\phi}_{vr} + \boldsymbol{\phi}_{vl}\right)\right] \\ &\quad + \mathbf{P}_w\left[\boldsymbol{\phi}_v^1 + \boldsymbol{\phi}_v^1 + \boldsymbol{\phi}_v^1 + \boldsymbol{\phi}_v^1 + 4\overline{\boldsymbol{\phi}} - 2\left(\boldsymbol{\phi}_{ur} + \boldsymbol{\phi}_{ul} + \boldsymbol{\phi}_{wr} + \boldsymbol{\phi}_{wl}\right)\right],\end{aligned}$$

$$\mathbf{P}_u = \mathbf{D}\mathbf{R}\hat{\mathbf{P}}_u\mathbf{R}^{-1}.$$

Because the coefficients, $\mathbf{L}_{iu}\left(i = 1, 2\right)$, are given by corner point fluxes, extra relations are needed for them. One can use the five point relations derived from the corner point leakage balance condition[4];

$$\mathbf{T}_{ij}^{C}\boldsymbol{\phi}_{ij}^{C} + \mathbf{T}_{ij}^{L}\boldsymbol{\phi}_{ij}^{L} + \mathbf{T}_{ij}^{R}\boldsymbol{\phi}_{ij}^{R} + \mathbf{T}_{ij}^{B}\boldsymbol{\phi}_{ij}^{B} + \mathbf{T}_{ij}^{T}\boldsymbol{\phi}_{ij}^{T} = \mathbf{q}_{ij}. \tag{35}$$

The subscript ij denotes one of the four corner points in the given node. $\boldsymbol{\phi}_{ij}^{s}\left(s = C, R, L, B, T\right)$ denotes the flux at the corner point designated by ij (s=C), and corner point fluxes at its right (s=R), its left (s=L), its bottom (s=B) and its top (s=T). The coefficients $\mathbf{T}_{ij}^{s}\left(s = C, R, L, B, T\right)$ and $\mathbf{q}_{ij}$ are defined in reference 4.

Equation (35) forms CPB equations and are extra relations to be solved in the AFEN option of the UNM formulation. The corner point fluxes from the solution of the CPB equations are used to determine the $\mathbf{L}_{iu}$ (i=0,1,2). For numerical enumeration, however, one must take precaution against the direct use of Eq. (34). Equation (34) is poorly conditioned because subtraction of large flux values is involved in determining the transverse leakage expansion coefficients that are smaller in numerical value by an order than fluxes. Therefore,

use of $\mathbf{L}_{iu}$ (i=0,1,2) determined directly from substituting large but inaccurate flux values from intermediate iteration stages into Eq. (34) may lead to erroneous results or fail to produce the converged solution. As will be discussed later, we face non-convergence difficulty in 3-D applications and fine-mesh UNM calculations of the AFEN option. This appears a drawback of the UNM formulation for the AFEN method. But the non-convergence difficulty can be easily avoided by enumerating $\mathbf{L}_{iu}$ using an under-relaxation scheme as follows;

$$\mathbf{L}_{iu}^{new} = \mathbf{L}_{iu}^{old} + \omega \left(\mathbf{L}_{iu} - \mathbf{L}_{iu}^{old} \right) \quad (i = 0,1,2) \tag{36}$$

where $\mathbf{L}_{iu}^{new}$ and $\mathbf{L}_{iu}^{old}$ are transverse leakage coefficients of the current and the previous steps, respectively. $\mathbf{L}_{iu}$ is the transverse leakage coefficients determined directly from Eq.(34) using flux values of the current step. ω (< 1) is the relaxation parameter.

Equations (31) and (32) in combination with Eqs. (25), (26), and (35) constitute a set of the basic nodal coupling relations in the UNM formulation. Except for Eq. (35), they are practically the same as those in the steady-state NEM formulation. In order to solve these relations, therefore, one can use the same iterative procedure introduced in reference 6 for NEM. Alternatively, one can utilize nonlinear coarse mesh finite difference (CMFD) schemes that are discussed in some detail in reference 5.

3. Numerical Results and Discussion

The UNM utilizes the transverse integration of the group diffusion equation while the AFEN method is not. Besides, the UNM above for the transient AFEN calculations differs from the transient AFEN method implemented recently by Kim et al.[3] Unlike their formulation which derives the intranodal flux distribution from the inhomogeneous 2-G diffusion equations similar to Eq. (2), the UNM formulation here derives it from the homogeneous 2-G diffusion equation as in the case of the static case. Consequently, the nodal coupling equations in the UNM formulation are of the same form regardless of the static and transient problems, even though the coupling coefficients change every time step. This as well as simplicity of nodal coupling relations may contribute to improved computational effectiveness of the UNM formulation for the transient AFEN calculations. In order to examine the computational effectiveness of the UNM formulation, we analyzed one of the well-known OECD/NEA transient benchmark problems designated as A1 transient problem. Figure 1 shows the OECD/NEA PWR core. The A1 problem is an octant core symmetry problem in which the transient is induced by the sudden withdrawal of the control rod located at the center of the core at the cold zero power. Table 1 shows the comparison of the UNM solutions of the AFEN option and several TINM solutions with reference solutions[7] in terms of initial steady state critical soluble boron concentration and 3-D power peak (F_q) and transient parameters such as power peak time and peak power. The NEM/QTL and the ANM/QTL are the NEM and the ANM solutions, respectively, with quadratic transverse leakage approximation (QTL). The ANM/ATL is the ANM solution with the analytic transverse leakage, Eq. (4), the expansion coefficients of which are determined in the same way as the QTL. There are two AFEN method solutions; AFEN/MSS and AFEN/CPB.

The AFEN/MSS denotes the AFEN solution in which corner point fluxes are obtained by the method of successive smoothing. In the AFEN/CPB solution, corner point fluxes are obtained from the CPB equation . The results of 1x1 radial node per assembly (N/A) calculations show that the AFEN/CPB is in better agreement with the 4x4 N/A reference solution than the three TINM calculations and the AFEN/MSS. The 2x2 N/A calculations enhance greatly the agreement of the three TINM and AFEN calculations with the reference results. The 2x2 N/A AFEN/CPB result appears the closest to the reference calculation. For further comparison, Figure 2 shows the transient core power excursion behavior with time. It is observed that the AFEN/CPB predicts more closely the transient core power excursion behavior predicted by the reference calculation. The last row of Table 1 compares the CPU times of the TINM and AFEN analysis of the A1 problem. Unlike the case of the TINM, the AFEN method requires solving the corner point balance equation. Because of this, the AFEN method takes longer CPU time than the TINM considered here.

4. Conclusion

The AFEN method formulation proposed recently for the transient reactor analysis has been tested in terms of 2-D transient problems only. Therefore, this paper may be the first-ever presentation on the performance of the AFEN method in terms of 3-D transient problems. As observed in the static applications, the results of OECD/NEA PWR transient problem A1 show that AFEN method outperforms the popular TINM in prediction accuracy at the expense of computational time. This encourages further tests of the UNM formulation here with many different 3-D transient problems.

References

1. Hyun Chul Lee and Chang Hyo Kim, “Unified Nodal Formulation for Analytic Function Expansion Nodal Method Solution to Two-Group Diffusion Equations in Rectangular Geometry,” Trans. Am. Nucl. Soc. 83, 409-411 (2000)
2. H. Finnemann, A. Galati, “NEACRP 3-D LWR Core Transient Benchmark – Final Specifications”, NEACRP-L-335 (Revision 1), January 1992.
3. D. S. Kim and N. Z. Cho, “The Kinetics Calculation in the Analytic Function Expansion Nodal Method with Galerkin Weighting,” ***Tran. Am. Nucl. Soc.*** (2000).
4. Jae Man Noh and N. Z. Cho, “A New Approach of Analytic Basis Function Expansion to Neutron Diffusion Nodal Calculation,” ***Nucl. Sci. Eng***. 116, 165 (1994).
5. Hyun Chul Lee and Chang Hyo Kim, “Unified Formulation of NEM and ANM Solutions to Two Group Diffusion Equations,” scheduled to be published in the 2001 June issue of ***Nucl. Sci. Eng***.
6. H. Finnemann, F. Bennewitz and M. R. Wagner, “Interface Current Techniques for Multidimensional Reactor Calculations,” ***Atomkernenergie***, **30**, 123-128 (1977).
7. M. P. Knight and P. Bryce, “Derivation of a Refined PANTHER Solution to the NEACRP PWR Rod-Ejection Transient,” Proc. Joint International Conference on Mathematical Methods and Supercomputing for Nuclear Applications, Vol. 1, Saratoga, 1997.

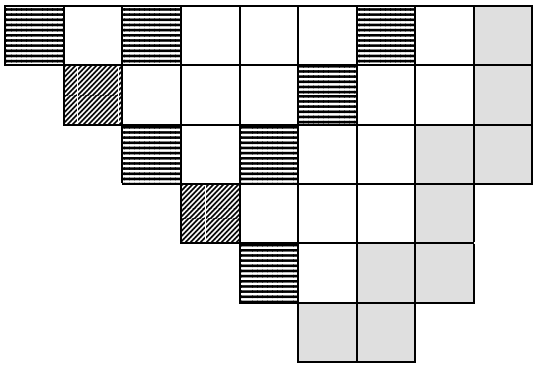

Figure 1. Core Configuration of OECD/NEA Transient Benchmark Problem Case A1

Table 1. UNM Analysis for OECD/NEA Transient Benchmark Problem Case A1

	4x4x36 N/FA		1x1x18 N/FA					2x2x18 N/FA				
	PAN-THER	ANM / QTL	NEM	ANM / QTL	ANM / ATL	AFEN / MSS	AFEN / CPB	NEM	ANM / QTL	ANM / ATL	AFEN / MSS	AFEN / CPB
Soluble Boron (ppm)	561.2	561.7	567.3	566.1	563.1	558.6	560.0	562.5	562.0	561.3	559.8	558.0
β_{eff}	2.8792	2.8787	2.8305	2.8482	2.8595	2.8836	2.8899	2.8693	2.8763	2.8782	2.8859	2.9368
Peak Power (%)	126.78	133.8	80.83	97.75	107.8	147.5	138.8	122.1	130.1	135.5	147.4	141.1
Peak Time (sec)	0.5375	0.5450	0.6975	0.6425	0.5975	0.5050	0.5200	0.5725	0.5575	0.5425	0.5150	0.5200
CPU Time (sec)	-	-	93	94	94	108	126	518	520	532	572	729

Time step : 465 steps

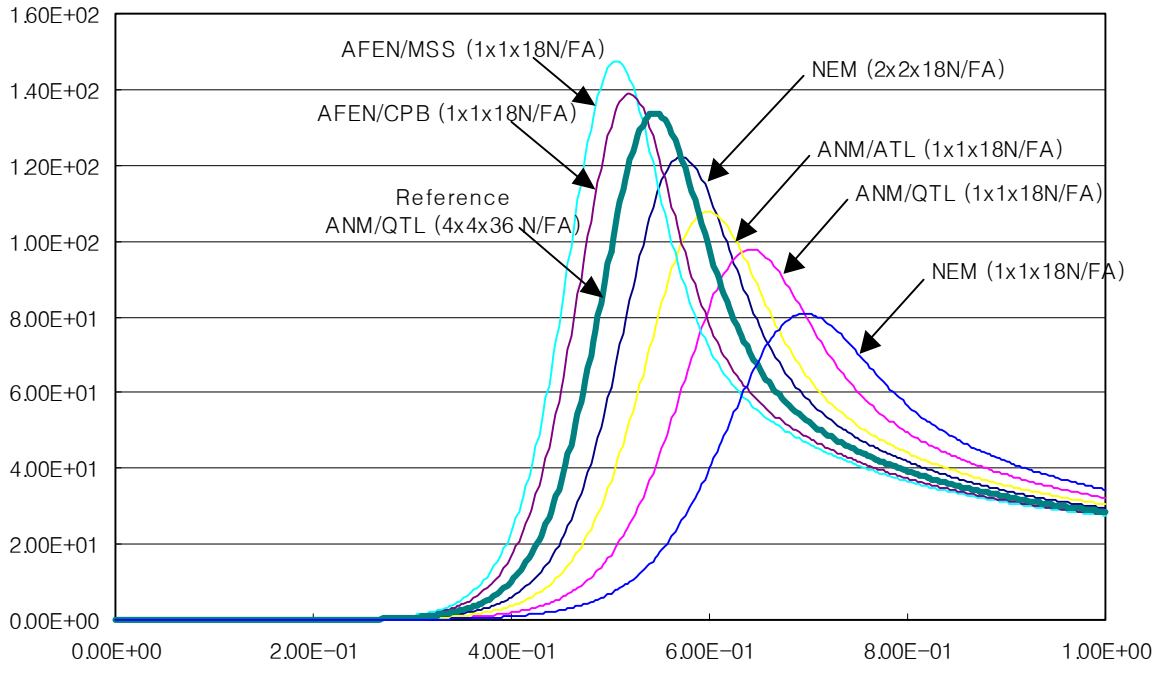

Figure 2. Core Power Excursion Behavior in OECD/NEA Transient Benchmark Problem Case A1